The paper was presented at the Tenth Meeting
"New Trends in Fatigue and Fracture" (NT2F10)
Metz, France, 30 August–1 September, 2010

Hamidréza Ramézani[1], *Jena Jeong*[2]

INFINITESIMAL NON-LINEAR COSSERAT THEORY BASED ON THE GRAIN SIZE LENGTH SCALE

INFINITEZIMALNA NELINEARNA TEORIJA KOSERA NA BAZI DUŽINSKE SKALE VELIČINE ZRNA

Original scientific paper
UDC: 666.971.4.019 : 519.6
Paper received: 31.01.2011

Author's address:
[1)] CRMD, UMR CNRS 6619- Research Center on Divided Materials, École Polytechnique de l'Université d'Orléans, France, hamidreza.ramezani@univ-orleans.fr
[2)] ESTP/IRC/LM-Lean Modeling-École Spéciale des Travaux Publics, du Bâtiment et de l'industrie (ESTP), 28 avenue du Président Wilson, 94234 Cachan cedex, France, jeong@profs.estp.fr

Keywords
- non-linear Cosserat theory
- 3D-FEM
- grain size
- Modified Brazilian Disk
- characteristic length scale

Ključne reči
- nelinearna teorija Kosera
- 3D MKE
- veličina zrna
- Modifikovani Brazilski Disk
- karakteristična dužinska skala

Abstract

A non-linear Cosserat theory involving the Arbitrary Lagrangian-Eulerian (ALE) method has been introduced into the brittle isotropic materials (amorphous glass and cement mortar) using the Modified Brazilian Disk (MBD) under an uni-axial compressive loading. These numerical experiments shed light on the nature of the Cosserat-based media and material moduli determination which are difficult to acquire using the most well-known experimental viewpoints. By using the identical micro-rotation constants ($\alpha = \beta = \gamma = \mu L_G^2$ and $\Psi = 2/3$), the Cosserat moduli reduce to only four constants for the 3D cases. According to the results obtained in this paper, the present methodology substantiates that the Cosserat theory would be readily applied to the wide range of materials from the full amorphous materials to the heterogeneous materials by changing the length scale parameter. Some fresh routes and new outlooks are discussed afterwards.

Izvod

Opisana je nelinearna teorija Kosera koja sadrži metodu proizvoljnog Lagranžijana-Ojlerijana (ALE), koja je primenjena kod krtih izotropnih materijala (amorfno staklo i cementni malter) primenom modifikovanog brazilskog diska (MBD) pri jednoosnom pritisnom opterećenju. Ovi numerički eksperimenti bacaju više svetlosti na prirodu medija tipa Kosera i na određivanje modula materijala, koji se nerado prihvataju s obzirom na dobro poznate eksperimentalne tačke gledišta. Korišćenjem identičnih mikro rotacionih konstanti ($\alpha = \beta = \gamma = \mu L_G^2$ i $\Psi = 2/3$), Kosera moduli se uprošćavaju na samo četiri konstante za 3D slučajeve. Prema rezultatima u ovom radu, sadašnja metodologija potkrepljuje da se Kosera teorija može opravdano primeniti na širok raspon materijala, od potpuno amorfnih materijala do heterogenih materijala, i to izmenom parametra dužinske skale. Data je diskusija nekih novih pravaca istraživanja i novih zapažanja.

INTRODUCTION

Development of Cosserat models, motivation and applications

This article addresses the general continuum models involving independent rotations which were introduced by Cosserat brothers /1/ at the beginning of the last century. Their original nonlinear and geometrically exact development has been widely forgotten for decades to be only rediscovered in a restricted linearized setting in the early sixties /2, 3, 4/. Since then, the original Cosserat concept has been generalized in various directions, notably by Eringen and his co-workers who extended the Cosserat concept to include also micro-inertia effects called 'micromorphic theory'[1]. The further simplified Cosserat theory can be obtained assuming that the macro-rotations are the same as the micro-rotations, which is named *couple stress theory* or so-called *indeterminate couple stress theory* /8, 9/ and some elastic-plastic applications would be also found out in /10/. The Cosserat model includes in a natural way size effect and is increasingly used to regularize non-well posed situation to analyze more efficiently the diagonal fracture plane under a compressive loading for the hetero-

[1] Some of Eringen's notations have been revised later on by Cowin /5/ and by Eringen himself /6, 7/. The original notations make some flaws and it should be carefully taken into account by the relevant Cosserat moduli or Cosserat material constants.

geneous materials, e.g. sand, soil /11, 12/ and granular materials using elasto-plasticity /13-21/. It is of importance to mention that the other groups have also obtained the micro-rotations of particles and their localizations on the shear bands via 2D numerical methods /22, 23/. The other applications are related to the artificial materials like foams /24-27/, cellular materials /28/ and some other outstanding contributions should be addressed such as /29-31/.

Unfortunately, the direct measurements of micro-rotation of particles are not achievable with high accuracy but we can measure the micro-rotation in the diagonal fracture plane by means of the stereophotometric method /32/. Lakes proposed an experimental procedure to find out four supplementary material parameters μ_c, α, β and γ for the Cosserat media /33/. However, his proposed experimental test is not easy to achieve and it is based upon linear Cosserat kinematics extracted by Gauthier et Jahsman /34, 35/ in the early seventies. The micropolar theory can be also used as a generalized continuum theory in which the microstructure detail can be averaged out by the "characteristic length scale" /8/ including some assumptions about the micro-rotation vector /36/. The latter parameter can be considered as the infinitesimal homogeneous region in the heterogeneous media and it is frequently used to model damage phenolmena in the concrete /37, 38/. Over the years, a variety of boundary value problems have been solved in terms of analytical expression which are then used for the determination of material moduli in the infinitesimal linear Cosserat model /39/. Notably, the solution of the pure torsion problem with prescribed torque at the end faces has been given /34, 35, 40/ and used for the determination of the length scales of different materials. Despite the huge effort spent in investigating the Cosserat model, two main drawbacks still controversially remain. These two points are: the problem of physical meaningful boundary or side-condition for the micro-rotation and physically consistent determintion of the Cosserat parameters.

Paper organization

In the present paper, we investigate and use the full Cosserat media or non-linear Cosserat media via our proposed characteristic length scale assumptions and the grain sizes. First we present the linear and non-linear Cosserat theory and parameters identification with respect to the semi-positive definiteness of the constitutive laws and local positivity of strain energy density or so called strongly ellipticity. Second, we focus on the problem of indirect tensile test known as Modified Brazilian Disk (MBD). We choose an amorphous material with very low porosity (glass of nano-scale pore size /41/) and a heterogeneous material with high porosity (cement mortar). The mentioned elastic brittle materials are analyzed in order to evaluate the average grain size as the characteristic length scale in the Cosserat theory. As will be discussed in the next sections, the Cosserat theory would be used to the classical theory, i.e. Cauchy-Boltzmann theory as well as granular materials.

MATHEMATICAL FORMULATION OF COSSERAT-BASED SOLIDS

This section does not contain any new result. Let us begin by establishing the coupled kinematical relations for the non-linear Cosserat models and their appropriate strain and curvature energy densities.

Cosserat theory kinematics

Classical kinematics or so-called linearized kinematics

The most essential matter in the Cosserat theory is the existence of the additional independent degree of freedoms, i.e. micro-rotation vector ($\phi \in \mathbb{R}^3$) besides the displacement vector ($u \in \mathbb{R}^3$) (Figure 1).

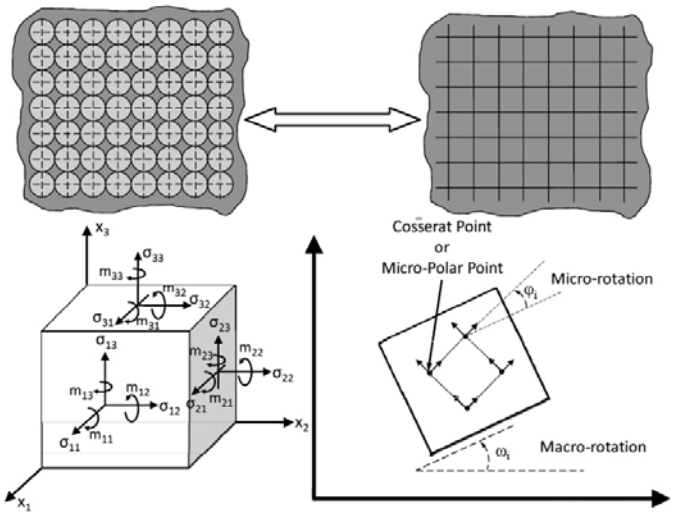

Figure 1. a) Modelling heterogeneous materials b) Components of stress and stress moment tensors in Cosserat theory, c) Micro-rotation compared to macro-rotation.
Slika 1. a) Modeliranje heterogenog materijala, b) Komponente tenzora napona i momenta napona - Kosera teorija c) Mikro-rotacija uporedjena sa makro-rotacijom

The main idea comes from the fact that one point in the continuum media is not a simple point. As a matter fact, this point is small enough to be considered as a point (infinitesimal) in the classical continuum mechanics and it is equally large enough to provide the micro-rotation (to be representative of the micro-structure in a statistical sense) /42/. Eringen took into account the above-mentioned vectors and established the following second-rank tensors /7/:

$$\bar{\varepsilon}^T := \nabla u - \bar{A}\,, \text{ where } \bar{A} := -e_{ijk}\phi_k \hat{e}_i \otimes \hat{e}_j \text{ and } \nabla u := (\nabla \otimes u)^T = u_{i,j}\hat{e}_i \otimes \hat{e}_j \text{ for } i,j,k = 1,2,3 \tag{1a}$$

$$\bar{k} := \nabla \phi\,, \text{ where } \nabla \phi := (\nabla \otimes \phi)^T = \phi_{i,j}\hat{e}_i \otimes \hat{e}_j \text{ for } i,j,k = 1,2,3 \tag{1b}$$

where

$\bar{\varepsilon} \in \mathbb{R}^3 \times \mathbb{R}^3$, $\nabla u \in \mathbb{R}^3 \times \mathbb{R}^3$, $\phi \in \mathbb{R}^3$, $\bar{A} \in \mathrm{SO}(3) \subset \mathbb{R}^3 \times \mathbb{R}^3$,

$e \in \mathbb{R}^3 \times \mathbb{R}^3 \times \mathbb{R}^3$ and $k \in \mathbb{R}^3 \times \mathbb{R}^3$ are first Cosserat stretch tensor, gradient of displacement vector, micro-rotation dual tensor, third-rank permutation tensor or Levi-Civita symbol and second-rank curvature tensor, respectively.

The above-depicted linearized kinematics provided by Eringen has been widely used to obtain the analytical solutions of the torsion test with the long circular Cosserat

bars /34/. The extracted analytical solutions by using the linearized kinematics as mentioned earlier are taken into account in determining the material constants, /33/.

Geometrically exact kinematics or so-called non-linear kinematics

Let's get started with the deformation gradient tensor definition for the modern mechanics (F). The deformation gradient F is a second-rank tensor; according to the polar decomposition theorem, a second rank tensor can be described as a product of a positive symmetric tensor (U, $V \in$ PSym(3)) with an orthogonal tensor ($R = polar[F] \in GL+(3)$), /43/. This decomposition can be performed by means of right decomposition as below:

$$F := RU = \bar{R}\bar{U} \tag{2}$$

By considering $\bar{U} \in \mathbb{R}^3 \times \mathbb{R}^3$, we can find out the first Cosserat stretch tensor known as $\bar{U} - \mathrm{ll}$ and we can write it again as follows:

$$\bar{E}^T := \bar{U} - \mathrm{ll} = \bar{R}^T F - \mathrm{ll} \tag{3a}$$

where $$\bar{R} = \exp(\bar{A}) = \mathrm{ll} + \frac{\bar{A}}{1!} + \frac{\bar{A}^2}{2!} + \frac{\bar{A}^3}{3!} + \ldots$$

where $$\bar{A} = \mathrm{anti}\,\phi = -\phi \cdot e = -e_{ijk}\phi_k \hat{e}_i \otimes \hat{e}_j \tag{3b}$$

or $$\bar{R} = \exp(\bar{A}) = \mathrm{ll} + \frac{\sin(\|\phi\|)}{\|\phi\|}\bar{A} + \frac{1-\cos(\|\phi\|)}{\|\phi\|^2}\bar{A}^2$$

where $$\phi = \mathrm{axl}\,\bar{A} = -\frac{1}{2}e : \bar{A} = -\frac{1}{2}e_{ijk}A_{jk}\hat{e}_i \tag{3c}$$

and $$F := \mathrm{ll} - \nabla u \tag{3d}$$

The Eqs. (3a), (3c) and (3d) prepare the first Cosserat stretch tensor in its geometrically exact or so-called non-linear case as:

$$\bar{E}^T := \bar{R}^T F - \mathrm{ll} = \left(\mathrm{ll} + \frac{\sin(\|\phi\|)}{\|\phi\|}\bar{A} + \frac{1-\cos(\|\phi\|)}{\|\phi\|^2}\bar{A}^2 \right)^T (\mathrm{ll} + \nabla u) - \mathrm{ll} \tag{4a}$$

or $$\bar{E}^T := \bar{R}^T F - \mathrm{ll} = \left(\cos(\|\phi\|)\,\mathrm{ll} + \frac{\sin(\|\phi\|)}{\|\phi\|}\bar{A} + \frac{1-\cos(\|\phi\|)}{\|\phi\|^2}\phi \otimes \phi \right)^T (\mathrm{ll} + \nabla u) - \mathrm{ll} \tag{4b}$$

We can further simplify Eq. (4a) and rewrite the first kinematical equation as below:

$$\bar{E}^T := \nabla u - \frac{\sin(\|\phi\|)}{\|\phi\|}\bar{A} - \frac{\sin(\|\phi\|)}{\|\phi\|^2}\bar{A}\nabla u + \frac{1-\cos(\|\phi\|)}{\|\phi\|^2}\bar{A}^2 + \frac{1-\cos(\|\phi\|)}{\|\phi\|^2}\bar{A}^2\nabla u \tag{5}$$

The curvature tensor or so-called wryness tensor $\bar{K}$ can be extracted in terms of several definitions for micro-rotation. Some fresh studies can be addressed in /44, 45/. As mentioned in /45/, there are many studies in which several techniques on how to describe the rotation group SO(3) are developed, Rooney /46/, Guo /47/, Pietraszkiewicz and Badur /48/, Altman /49/, Atluri and Cazzani /50/, Borri et al. /51/, Geradin and Cardona /52/ and Chroscielewski et al. /53/[2]. General definition for wryness or curvature tensor can be written as below /54, 55, 56/:

$$\bar{K}^T := -\frac{1}{2}e : (R^T \nabla \otimes R) \tag{6}$$

where, $\bar{K} \in \mathbb{R}^3 \times \mathbb{R}^3$, $e \in \mathbb{R}^3 \times \mathbb{R}^3 \times \mathbb{R}^3$, $R \in SO(3) \subset \mathbb{R}^3 \times \mathbb{R}^3$ and $\nabla R \in \mathbb{R}^3 \times \mathbb{R}^3 \times \mathbb{R}^3$ are curvature tensor, Levi-Civita symbol, proper orthogonal micro-rotation tensor and gradient of orthogonal micro-rotation tensor, respectively. There are seven natural Lagrangian curvature tensors or so-called wryness tensors for different finite rotation vectors /45/. The use of other forms like those done by Münch /55/ and Sansour /56/ would sustain some numerical discrepancies during the computations. By taking advantage of the relation proposed by Pietraszkiewicz and Eremeyev., i.e. $\phi \in [-2\pi, 2\pi]$, the above-defined curvature tensor can be written as below:

$$\bar{K}^T := \left(\frac{\sin(\|\phi\|)}{\|\phi\|}\mathrm{ll} + \frac{\|\phi\| - \sin(\|\phi\|)}{\|\phi\|^3}\phi \otimes \phi - \frac{1-\cos(\|\phi\|)}{\|\phi\|^2}\bar{A} \right)\nabla\phi \tag{7a}$$

or

$$\bar{K}^T := \frac{2\sin(\|\phi\|) - \|\phi\|}{\|\phi\|}\nabla\phi - \frac{1-\cos(\|\phi\|)}{\|\phi\|^2}\bar{A}\nabla\phi + \frac{\|\phi\| - \sin(\|\phi\|)}{\|\phi\|^3}\bar{A}^2\nabla\phi \tag{7b}$$

Therefore, we can summarize the constitutive laws for non-linear Cosserat theory as below:

$$\bar{E}^T := \nabla u - \frac{\sin(\|\phi\|)}{\|\phi\|}\bar{A} - \frac{\sin(\|\phi\|)}{\|\phi\|}\bar{A}\nabla u + \frac{1-\cos(\|\phi\|)}{\|\phi\|^2}\bar{A}^2 + \frac{1-\cos(\|\phi\|)}{\|\phi\|^2}\bar{A}^2\nabla u \tag{8a}$$

$$\bar{K}^T := \frac{2\sin(\|\phi\|) - \|\phi\|}{\|\phi\|}\nabla\phi - \frac{1-\cos(\|\phi\|)}{\|\phi\|^2}\bar{A}\nabla\phi + \frac{\|\phi\| - \sin(\|\phi\|)}{\|\phi\|^3}\bar{A}^2\nabla\phi \tag{8b}$$

By neglecting the non-linear phrases in terms of ∇u and $\bar{A}$ and assuming small deformation ($\sin(\|\phi\|)/\|\phi\| = 1$ and $(2\sin(\|\phi\|) - \|\phi\|)/\|\phi\| = 1$ when $\|\phi\| \to 0$), we infer the Eringen's simplified kinematics or so-called linear kinematics (Eqs. (1a) and (1b)). In the present study, we incorporate recently-explored strain energy densities into

[2] These parameterizations can roughly be classified as vectorial and non-vectorial ones. Various finite rotation vectors as well as the Cayley-Gibbs and exponential map parameters are examples of the vectorial parameterization, for they all have three independent scalar parameters as Cartesian components of a generalized vector in the 3D vector space (see /44/ and /45/ for more detail).

the Cosserat-based media involving the Arbitrary Lagrangian Eulerian (ALE) moving mesh method /57/[3]. In the next sub-sections, we review the anisotropic and isotropic constitutive laws including and excluding the centro-symmetric postulates for the continuum mechanics. However, we concentrate on the centro-symmetric materials for our numerical experiments in the current study.

Total strain energy density concept and their corresponding constitutive laws

For a non-linear or so-called geometrically exact elastic Cosserat solids, a total strain energy density function can be expressed as a polynomial in function of $\bar{E}$ and $\bar{K}$ based on the expansion power series theory:

$$W(\bar{E},\bar{K}) = W_{\text{mp}}(\bar{E},\bar{K}) + W_{\text{cs}}(\bar{E},\bar{K}) + W_{\text{curv}}(\bar{E},\bar{K}) \quad (9a)$$

$$W_{\text{mp}}(\bar{E},\bar{K}) = W^0_{\text{mp}} + \mathbf{S}:\bar{E} + \frac{1}{2}\bar{E}:\mathbf{D}:\bar{E} \quad (9b)$$

$$W_{\text{cs}}(\bar{E},\bar{K}) = W^0_{\text{cs}} + \frac{1}{2}\bar{E}:\mathbf{C}:\bar{K} + \frac{1}{2}\bar{K}:\mathbf{C}:\bar{E} = W^0_{\text{cs}} + \bar{E}:\mathbf{C}:\bar{K} \quad (9c)$$

$$W_{\text{curv}}(\bar{E},\bar{K}) = W^0_{\text{curv}} + \mathbf{B}:\bar{K} + \frac{1}{2}\bar{K}:\mathbf{E}:\bar{K} \quad (9d)$$

Centro-symmetric case: anisotropic and isotropic constitutive laws

In the absence of initial energy densities, stress and couple stress ($W^0_{\text{mp}} = W^0_{\text{cs}} = W^0_{\text{curv}} = 0$ and $\mathbf{S} = \mathbf{B} = \mathbf{0}$) and the hypothesis of centro-symmetry effects for the Cosserat media ($\mathbf{C} = \mathbf{0}$), we can find the following anisotropic constitutive equations:

$$\bar{\sigma} = \frac{\partial W(\bar{E},\bar{K})}{\partial \bar{E}} = \mathbf{D}:\bar{E} \quad \text{or} \quad \bar{\sigma}_{ij} = D_{ijkl}\bar{E}_{kl} \quad \text{for } i,j,k,l = 1,2,3 \quad (10a)$$

and

$$m = \frac{\partial W(\bar{E},\bar{K})}{\partial \bar{K}} = \mathbf{E}:\bar{K} \quad \text{or} \quad \bar{K}_{ij} = E_{ijkl}\bar{K}_{kl} \quad \text{for } i,j,k,l = 1,2,3 \quad (10b)$$

By applying isotropy property for the stiffness and curvature stiffness fourth-rank tensors, one can find out the following relations:

$$\bar{\sigma} = 2\mu\,\text{sym}\,\bar{E} + 2\mu_c\,\text{skew}\,\bar{E} + \lambda\,\text{tr}[\bar{E}]\,\text{ll}$$

$$\text{or} \quad \bar{\sigma} = (\mu+\mu_c)\bar{E} + (\mu-\mu_c)\bar{E}^T + \lambda\,\text{tr}[\bar{E}]\,\text{ll} \quad (11)$$

and

$$m = \beta\bar{K}^T + \gamma\bar{K} + \alpha\,\text{tr}[\bar{K}]\,\text{ll} \quad \text{or}$$

$$m = (\gamma+\beta)\,\text{sym}\,\bar{K} + (\gamma-\beta)\,\text{skew}\,\bar{K} + \alpha\,\text{tr}[\bar{K}]\,\text{ll} \quad (12a)$$

or

$$m = (\gamma+\beta)\,\text{devsym}\,\bar{K} + (\gamma-\beta)\,\text{skew}\,\bar{K} + \frac{3\alpha+(\beta+\gamma)}{2}\,\text{tr}[\bar{K}]\,\text{ll} \quad (12b)$$

[3] In this method, the mesh movement follows the movement of physical material and it is very useful in solid mechanics involving relatively large deformation. It is of great importance to remind that for very large deformation, it is more beneficial to re-mesh the FEM model. This matter removes mesh distortion drawback during the computations.

λ and μ are the classical Lamé's constants and μ_c, α, β and γ are new additional material parameters introduced into Cosserat theory.

By taking advantage of the isotropy of the constitutive laws as mentioned earlier, we can rewrite the strain energy density and curvature energy density as below:

– strain energy density

$$W_{\text{mp}}(\bar{E}) = \mu\left\|\text{sym}\,\bar{E}\right\|^2 + \mu_c\left\|\text{skew}\,\bar{E}\right\|^2 + \frac{\lambda}{2}\text{tr}^2[\bar{E}]$$

$$= \mu\left\|\text{devsym}\,\bar{E}\right\|^2 + \mu_c\left\|\text{skew}\,\bar{E}\right\|^2 + \frac{3\lambda+2\mu}{6}\text{tr}^2[\bar{E}] \quad (13a)$$

$$= \frac{1}{2}\left(\lambda\,\text{tr}^2[\bar{E}] + (\mu+\mu_c)\left\|\bar{E}\right\|^2 + (\mu-\mu_c)\,\text{tr}[\bar{E}^2]\right)$$

– curvature energy density

$$W_{\text{curv}}(\bar{K}) = \frac{\gamma+\beta}{2}\left\|\text{sym}\,\bar{K}\right\|^2 + \frac{\gamma-\beta}{2}\left\|\text{skew}\,\bar{K}\right\|^2 + \frac{\alpha}{2}\text{tr}^2[\bar{K}]$$

$$= \frac{\gamma+\beta}{2}\left\|\text{devsym}\,\bar{K}\right\|^2 + \frac{\gamma-\beta}{2}\left\|\text{skew}\,\bar{K}\right\|^2 + \frac{3\alpha+(\beta+\gamma)}{6}\text{tr}^2[\bar{K}] \quad (13b)$$

$$= \frac{1}{2}\left(\alpha\,\text{tr}^2[\bar{K}] + \gamma\left\|\bar{K}\right\|^2 + \beta\,\text{tr}[\bar{K}^2]\right)$$

By using of the mathematical points of view, the strain energy density $W_{\text{mp}}(\bar{E};\bar{K})$ and the curvature energy density $W_{\text{curv}}(\bar{E};\bar{K})$ would have the local positivity condition. But that is not sufficed and the semi-positive definiteness of fourth-rank stiffness tensors of constitutive laws would be required either /58/:

$$\begin{aligned} &\mu \geq 0,\ 3\lambda+2\mu \geq 0,\ \mu_c \geq 0 \\ &\beta+\gamma \geq 0,\ 3\alpha+(\beta+\gamma) \geq 0,\ \gamma-\beta \geq 0,\ \gamma \geq 0 \end{aligned} \quad (14)$$

Traditionally, the four supplementary material parameters, i.e., μ_c, α, β and γ can be expressed by the other terms, ℓ_b, ℓ_t, N, Ψ /33/[4].

Equilibrium equations

In the absence of macro and micro-accelerations the equilibrium equations of the Cosserat theory are given as below under weak form formulation:

$$\int_{\Omega(t)}(\bar{\sigma}_{ji,j} + \rho b_i)\,dV = 0 \quad \text{for } i,j = 1,2,3 \text{ on } \Omega(t) \in \mathbb{R}^3 \times]0,T] \quad (16a)$$

$$\int_{\Omega(t)}(m_{ji,j} - e_{ijk}\bar{\sigma}_{jk} + \rho c_i)\,dV = 0 \quad i,j = 1,2,3 \text{ on } \Omega(t) \in \mathbb{R}^3 \times]0,T] \quad (16b)$$

[4] They represent the characteristic length scale for bending, characteristic length scale for torsion, coupling number and polar ratio, respectively.

The above-defined so-called material parameters have been substantially applied for determining the Cosserat material constants, notably by Lakes /59, 40, 60/. The previously indicated Cosserat moduli (μ_c, α, β and γ) could be denoted as below /61/:

$$\ell_b^2 := \frac{\gamma}{2(2\mu^*+\kappa)} \quad \text{and} \quad \ell_t^2 := \frac{\beta+\gamma}{2\mu^*+\kappa} \quad (15a)$$

$$N^2 := \frac{\mu_c}{\mu+\mu_c} = \frac{\kappa}{2(\mu^*+\kappa)} \quad \text{where} \quad 0 \leq N^2 \leq 1 \quad (15b)$$

$$\Psi := \frac{\beta+\gamma}{\alpha+\beta+\gamma} \quad \text{where} \quad 0 \leq \Psi \leq \frac{3}{2} \quad (15c)$$

where, κ and μ^* stand for the Cosserat couple modulus and Pseudo-Lamé's constant in accordance with Eringen's notation.

(16a) and (16b) imply that stress tensor $\bar{\sigma}_{ij}$ is not necessarily symmetric and its antisymmetric part is determined by the divergence of the couple stress tensor m_{ij} or so-called stress moment. These equations ((16a) and (16b)) are the outcome of the virtual work principle on deformable solids, /62/.

ANALYTICAL EVALUATION OF MATERIAL PARAMETERS IN MICROPOLAR THEORY AND CHARACTERISTIC LENGTH

General considerations

As explained earlier, the non-linear kinematics in conjunction with the ALE method are used into 3D-FEM calculations. This issue unwillingly produces the non-linear computations and the runtime would last more than those carried out for the linear Cosserat elasticity. This matter is entirely different from the material non-linearities issue in which the non-linear analyses are required. It is well worth noting that the authors use the most complete kinematics (geometrically exact) which is originally proposed by Cosserat brothers in early 1909, involving ALE moving mesh method. These features help us to carry out the FEM simulations as far as possible close to the original kinematics or realistic case. Anyway, in the practical engineering applications, linear Cosserat theory is quite adequate in describing the deformations (small deformation issue). We fix the relative error to 1×10^{-6} for all computations herein. The mesh independency issue has been evaluated for our computations either.

Analytical evaluation of curvature energy density using nullspace theory

Before getting started with non-linear Cosserat theory, it is apt to emphasize the curvature energy density classifications using Toupin's parameter /8/, i.e. characteristic length scale L_c as below, /63/:

Linear Cosserat theory

This case is well investigated by first author /58, 63, 64/ and it is numerically studied in /65, 66/ by the authors:

- **Point-wise case** called **case1** /55/: This case corresponds to $\alpha = 0$, $\beta = 0$ and $\gamma = \mu L_c^2$

$$W_{\text{curv}}(\bar{k}) := \frac{\mu L_c^2}{2} \bar{k} : \bar{k} = \frac{\mu L_c^2}{2} \left\| \bar{k} \right\|^2 \tag{17}$$

  – **Deviatoric point-wise case**, /67/: This case corresponds to $\alpha = -\mu L_c^2/3$, $\beta = 0$ and $\gamma = \mu L_c^2$

$$W_{\text{curv}}(\bar{k}) := \frac{\mu L_c^2}{2} \text{dev}\bar{k} : \text{dev}\bar{k} = \frac{\mu L_c^2}{2} \left\| \text{dev}\bar{k} \right\|^2 = \\ = \frac{\mu L_c^2}{2} \left(\left\| \bar{k} \right\|^2 - \frac{1}{3} \text{tr}^2[\bar{k}] \right) \tag{18}$$

- **Symmetric case** called **case2** /68-71/: This case corresponds to $\alpha = 0$ and $\beta = \gamma = \mu L_c^2/2$

$$W_{\text{curv}}(\bar{k}) := \frac{\mu L_c^2}{2} \text{sym}\bar{k} : \text{sym}\bar{k} = \frac{\mu L_c^2}{2} \left\| \text{sym}\bar{k} \right\|^2 = \\ = \frac{\mu L_c^2}{2} \left(\frac{1}{2} \left\| \bar{k} \right\|^2 + \frac{1}{2} \text{tr}[\bar{k}^2] \right) \tag{19}$$

- **Conformal case** called **case3** /63, 65, 72, 73/: This case corresponds to $\alpha = -\mu L_c^2/3$ and $\beta = \gamma = \mu L_c^2/2$

$$W_{\text{curv}}(\bar{k}) := \frac{\mu L_c^2}{2} \text{devsym}\bar{k} : \text{devsym}\bar{k} = \frac{\mu L_c^2}{2} \left\| \text{devsym}\bar{k} \right\|^2 = \\ = \frac{\mu L_c^2}{2} \left(\frac{1}{2} \left\| \bar{k} \right\|^2 + \frac{1}{2} \text{tr}[\bar{k}^2] - \frac{1}{3} \text{tr}^2[\bar{k}] \right) \tag{20}$$

- **Symmetric case with non-negative α** called **case4**: This case corresponds to $\alpha = \beta = \gamma$ and $\gamma = \mu L_c^2$

$$W_{\text{curv}}(\bar{k}) := \frac{\mu L_c^2}{2} \left(\bar{k} : \bar{k} + \bar{k}^T : \bar{k} + \text{tr}[\bar{k}]^2 \right) = \\ = \frac{\mu L_c^2}{2} \left(\left\| \bar{k} \right\|^2 + \text{tr}[\bar{k}^2] + \text{tr}^2[\bar{k}] \right) \tag{21}$$

Non-linear Cosserat theory

The curvature strain energy density for non-linear kinematics or so-called geometrically exact has been described in function of $\hat{K} := R^T \text{Curl}_{\#}[R]$ /74, 55/ and it is related to the curvature tensor or wryness tensor by the following equation /74, 55/:

$$\hat{K} = \bar{K} - tr[\bar{K}] \text{ll} \tag{22}$$

$\text{Curl}_{\#}[R] \in \mathbb{R}^3 \times \mathbb{R}^3$, $R \in SO(3) \subset \mathbb{R}^3 \times \mathbb{R}^3$, and $\bar{K} \in \mathbb{R}^3 \times \mathbb{R}^3$ are row wise curl of proper orthogonal micro-rotation tensor, proper micro-rotation tensor and curvature tensor or wryness tensor, respectively. Correspondingly, we can rewrite different curvature energy densities as below:

- **Point-wise case** called **case1** /55/: This case corresponds to $\alpha = \mu L_c^2$, $\beta = 0$ and $\gamma = \mu L_c^2$:

$$W_{\text{curv}}(\bar{K}) := \frac{\mu L_c^2}{2} \left\| R^T \text{Curl}_{\#}[R] \right\|^2 = \frac{\mu L_c^2}{2} \left\| \hat{K} \right\|^2 \\ = \frac{\mu L_c^2}{2} \left(\left\| \bar{K} \right\|^2 + \text{tr}^2[\bar{K}] \right) \tag{23}$$

  – **Deviatoric point-wise case**, /67/: This case corresponds to $\alpha = -\mu L_c^2/3$, $\beta = 0$ and $\gamma = \mu L_c^2$:

$$W_{\text{curv}}(\bar{K}) := \frac{\mu L_c^2}{2} \left\| \text{dev}(R^T \text{Curl}_{\#}[R]) \right\|^2 = \frac{\mu L_c^2}{2} \left\| \text{dev}\hat{K} \right\|^2 = \\ = \frac{\mu L_c^2}{2} \left\| \text{dev}\bar{K} \right\|^2 = \frac{\mu L_c^2}{2} \left(\left\| \bar{K} \right\|^2 - \frac{1}{3} \text{tr}^2[\bar{K}] \right) \tag{24}$$

- **Symmetric case** called **case2** /68-71/: This case corresponds to $\alpha = \mu L_c^2$ and $\beta = \gamma = \mu L_c^2/2$:

$$W_{\text{curv}}(\bar{K}) := \frac{\mu L_c^2}{2} \left\| \text{sym}(R^T \text{Curl}_{\#}[R]) \right\|^2 = \frac{\mu L_c^2}{2} \left\| \text{sym}\hat{K} \right\|^2 = \\ = \frac{\mu L_c^2}{2} \left(\frac{1}{2} \left\| \bar{K} \right\|^2 + \frac{1}{2} \text{tr}[\bar{K}^2] + \text{tr}^2[\bar{K}] \right) \tag{25}$$

- **Conformal case** called **case3** /63, 65, 72, 73/: This case corresponds to $\alpha = -\mu L_c^2/3$ and $\beta = \gamma = \mu L_c^2/2$:

$$W_{\text{curv}}(\bar{K}) := \frac{\mu L_c^2}{2} \left\| \text{devsym}(R^T \text{Curl}_{\#}[R]) \right\|^2 = \frac{\mu L_c^2}{2} \left\| \text{devsym}\hat{K} \right\|^2 = \\ = \frac{\mu L_c^2}{2} \left(\frac{1}{2} \left\| \bar{K} \right\|^2 + \frac{1}{2} \text{tr}[\bar{K}^2] - \frac{1}{3} \text{tr}^2[\bar{K}] \right) \tag{26}$$

- **Symmetric case with non-negative α** called **case4**: This case corresponds to $\alpha = \beta = \gamma$ and $\gamma = \mu L_c^2$

$$W_{\text{curv}}(\bar{K}) := \frac{\mu L_c^2}{2}\left(\bar{K} : \bar{K} + \bar{K}^T : \bar{K} + \text{tr}[\bar{K}]^2\right) = \\ = \frac{\mu L_c^2}{2}\left(\|\bar{K}\|^2 + \text{tr}[\bar{K}^2] + \text{tr}^2[\bar{K}]\right) \quad (27)$$

The comparison among the cases for both linear and non-linear Cosserat theories substantiates that case1-deviatoric, case3-conformal case and case4 remain unchanged. Only the point-wise and symmetric cases (case1 and case2) take different configurations in the curvature energy density framework (Table 1). It is well worth noting that case 4 is conventionally defined and it is trivial that case4 retains the same feature explained earlier (linear Cosserat theory).

Table 1. Comparison among various curvature energy density cases for linear and non-linear Cosserat theories.
Tabela 1. Poređenje raznih slučajeva gustine krivolinijske energije za linearnu i nelinearnu teoriju Kosera.

Case No. and description	Linear Cosserat theory	Non-linear Cosserat theory
Case1-Pointwise case	$\alpha = 0$, $\beta = 0$ and $\gamma = \mu L_c^2$	$\alpha = \mu L_c^2$, $\beta = 0$ and $\gamma = \mu L_c^2$
Case1-Deviatoric case	$\alpha = -\mu L_c^2/3$, $\beta = 0$ and $\gamma = \mu L_c^2$	$\alpha = -\mu L_c^2/3$, $\beta = 0$ and $\gamma = \mu L_c^2$
Case2-Symmetric case	$\alpha = 0$ and $\beta = \gamma = \mu L_c^2/2$	$\alpha = \mu L_c^2$ and $\beta = \gamma = \mu L_c^2/2$
Case3-Conformal case	$\alpha = -\mu L_c^2/3$ and $\beta = \gamma = \mu L_c^2/2$	$\alpha = -\mu L_c^2/3$ and $\beta = \gamma = \mu L_c^2/2$
Case4-Non-negative α	$\alpha = \beta = \gamma$ and $\gamma = \mu L_c^2$	$\alpha = \beta = \gamma$ and $\gamma = \mu L_c^2$

Characteristic length scale L_c determination

Characteristic length scale overview

In the present study, we pay attention to case4 which provides symmetric stress moments like case2. The above-described cases reduce the six material moduli to only four material moduli, i.e. λ, μ, L_c and μ_c. The most salient point of Cosserat theory is to determine these parameters. Traditionally, we take μ_c equal to μ in the Cosserat simulations. However, the determination of L_c is not easy and several propositions pertaining to the L_c could be found out in the open literature:

1. Gauthier and Jahsman suggested two characteristic length scales known as ℓ_b and ℓ_t which deal with bending and torsion characteristic length scales /34, 35, 75/. These characteristic length scales come from the analytical solution of the linear Cosserat elasticity and they are widely applied by R.S. Lakes /33/. The original characteristic length scales have been extracted via long Cosserat bars under pure torsion. Determination of these parameters is very difficult and they are basically obtained from linear Cosserat theory.
2. Bazant proposed L_c nearly 2.7 times the largest aggregate in concrete /76, 37/ in the early eighties and his idea is followed by several papers in the concrete and cement society /38/.
3. Forest et al. applied the de Borst's assumption (case2-symmetric case) /70/ for 2D models i.e. $\alpha = 0$ and $\beta = \gamma$. They defined the characteristic length scale $L_c = \sqrt{\beta/\mu}$ using aluminium SiC metal matrix composite /77/. L_c value was considered between 10^{-4} and 10^2 mm.
4. Zhang et al. studied the Cosserat materials with Voronoi cell via FEM experiments /30/. They used three L_c values ($L_c = 0.01$ mm, $L_c = 0.1$ and $L_c = 1.0$ mm). Based upon their studies, the size effect was captured while they increased L_c in their linear 2D-FEM Cosserat models. The same methodology has been neatly applied to the elastic-plastic Cosserat materials by the abovementioned authors for granular materials /78/.

Definitions of characteristic lengths and our assumptions

Regarding the stress-strain and stress moment-curvature tensor relations (constitutive laws), two sets of material constants or so-called Cosserat moduli should be taken into account. Due to the dimensional difference between the two sets of parameters, at least three intrinsic characteristic lengths can be defined for an isotropic elastic micropolar material. These characteristic lengths can be denoted as:

$$L_{c_1}^2 := \frac{\alpha}{\mu},\ L_{c_2}^2 := \frac{\beta}{\mu} \text{ and } L_{c_3}^2 := \frac{\gamma}{\mu} \quad (28)$$

As previously discussed, six Cosserat material parameters should be deemed for 3D-models, i.e. (λ, μ, μ_c, α, β, and γ). These parameters can be described as (λ, μ, μ_c, L_{c1}, L_{c2} and L_{c3}). By taking advantage of the classical notations for Cosserat theory and fixing μ_c ($\mu_c = \mu$), we attain the following relations:

$$\Psi := \frac{\beta+\gamma}{\alpha+\beta+\gamma} = \frac{L_{c_2}^2 + L_{c_3}^2}{L_{c_1}^2 + L_{c_2}^2 + L_{c_3}^2} \quad (29a)$$

and

$$N^2 = \frac{\mu_c}{\mu+\mu_c} = \frac{1}{2} \quad (29b)$$

Assuming that L_{c1}, L_{c2} and L_{c3} deal with three diameters of an ellipsoid grain as illustrated in Fig. 2, the characteristic length scales can be re-written as below:

$$L_{c_1} = 2a,\ L_{c_1} = 2b \text{ and } L_{c_1} = 2c \quad (30)$$

If three characteristic length scales become identical, the ellipsoid shapes can be transformed to the spherical ones. Moreover, the aforementioned assumption coincides with case 4 (symmetric case with non-zero α). In the next section, we shall apply this curvature energy density configuration for our non-linear Cosserat models involving ALE method.

3D NUMERICAL SIMULATION OF THE ISOTROPIC NON-LINEAR COSSERAT THEORY

As explained previously, the equality of characteristic length scale ($\alpha = \beta = \gamma = \mu L_G^2$ where L_G is mean value of grain diameter for the granular materials) leads to case 4. Therefore, it is essential to substantiate the stiffness boundedness property for case4 by means of the M_T–Log(L_c) diagram. This semi-logarithmic diagram is utilized to prove that the mentioned case is physically feasible, i.e. it yields

the size effect in the sense that smaller specimens are stiffer than larger ones /65/. This matter has been investigated for linear Cosserat elasticity in /62/ via torsion test of a Cosserat bar. It is of great importance to remind that other cases have been taken into account in another study and they are out of scope of the present study.

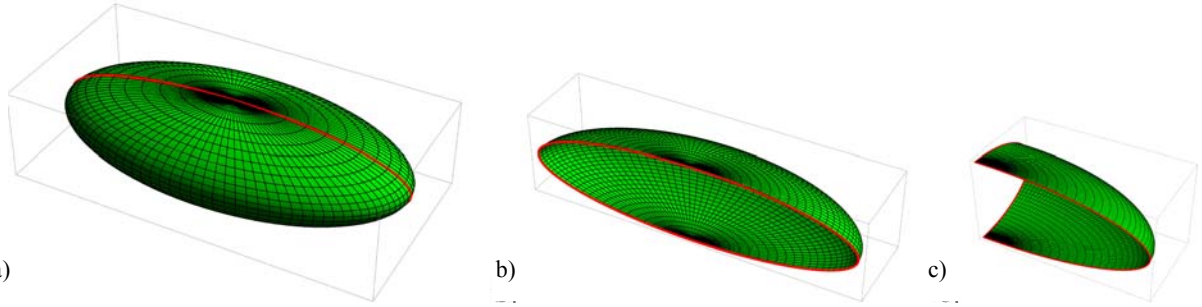

a) b) c)

Figure 2. Typical illustration of the ellipsoid grains assumption including the characteristic length scales (length=2a, width=2b and height=2c), a) Full ellipsoid, b) One-half ellipsoid, c) One-quarter ellipsoid.

Slika 2. Tipična ilustracija pretpostavke elipsoidnih zrna sa karakterističnim razmerama dužina (dužina=2a, širina=2b i visina=2c), a) potpuni elipsoid, b) polu-elipsoid, c) četvrtina elipsoida.

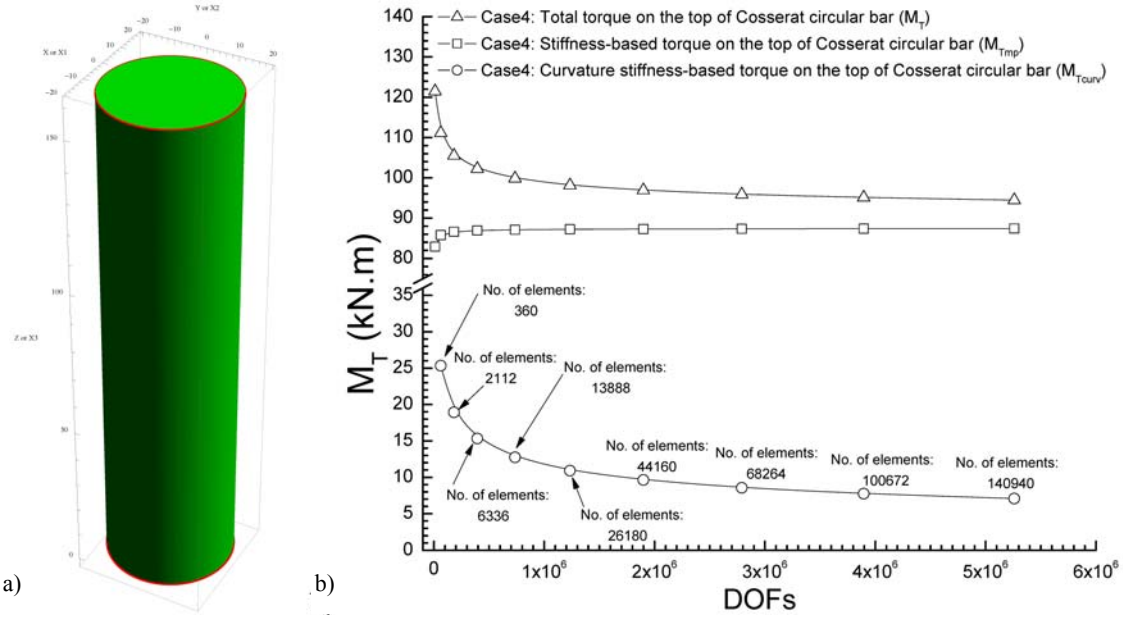

a) b)

Figure 3. Mesh independency evaluation of the non-linear Cosserat elasticity involving ALE for the circular Cosserat bar including E=30 GPa, ν=0.28, μ_c=μ, L_c=1E8 mm and finite rotation along x_3 axis υ=10°. a) Geometrical configuration of Cosserat bar (diameter=40 mm, length=160 mm), b) Torque versus DOFs curve for the symmetric case with non-zero α or case4 by steadily growing element number from 360 to 190720 elements (ansatz quadratic and linear Lagrange shape functions providing 28-node hexahedral solid elements) and up to 5259747 DOFs including Lagrange multiplier DOFs.

Slika 3. Proračun nezavisnom mrežom nelinearne Kosera elastičnosti sa ALE za kružni Kosera štap sa E=30 GPa, ν=0,28, μ_c=μ, L_c=1E8 mm i konačnom rotacijom za υ=10° duž ose x_3. a) Geometrijska konfiguracija Kosera štapa (prečnik=40 mm, dužina=160 mm), b) Moment u funkciji stepeni slobode za simetričan slučaj sa ne-nultim α ili slučaj4 pri laganom porastu broja elemenata od 360 do 190720 (počev od kvadratnih i linearnih funkcija oblika Lagranža sa 28-čvornih heksaedarskih punih elemenata) pa do 5259747 stepeni slobode uključujući i Lagranžove koeficijente stepeni slobode.

As it is well-known, the most Cosserat effect occurs when one sample is under pure torsion. Due to this fact, we chose the torsion test as a relevant tool to investigate our non-linear Cosserat models. As pointed out previously, to achieve the torsion test, the geometrically-exact angle of rotation should be applied on the top of specimen and after that, we integrate over the top of specimen for extracting the moment of torsion (see /65, 66/ for more detail). The total moment of torsion about the e_3-axis at the top of specimen consists of stiffness-based as well as curvature stiffness-based counterpart /64/:

$$M_T := \overbrace{\int_{\partial\Omega_{\mathrm{Top}}} (x\bar{\sigma}_{32} - y\bar{\sigma}_{31})dxdy}^{M_{\mathrm{Tmp}}:=\text{stiffness-based torque}} + \overbrace{\int_{\partial\Omega_{\mathrm{Top}}} m_{33}dxdy}^{M_{\mathrm{Tcurv}}:=\text{curvature stiffness-based torque}} \quad (31)$$

The mesh-independency issue is essential when we treat the size effect in the generalized continua, e.g. Micro-dilatation, Cosserat, Micro-stretch and Micro-morphic media. To handle it, the MT versus No. of DOFs is plotted by constantly growing the mesh density from very coarse mesh (11304 DOFs) to extremely fine (5259747 DOFs) (Fig. 3)

3D-FEM simulation of Modified Brazilian Disk specimens

In the present study, we consider two different elastic brittle materials, i.e. float glass and cement mortar (Table 2). In Fig. 4, the Scanning Electronic Microscopic (SEM) images for both materials are shown. Particularly, we focus on the indirect tensile stresses around the central hole of MBD samples /79/.

The uni-axial compression Brazilian test is commonly used on brittle materials to apply the compression at top of the disk specimen. This loading condition can provide indirect tensile stress in the direction of the median plane. The MBD consists of one small central hole (a = 30 mm diameter) on the outer disk of diameter and thickness 150 mm (= D) and 100 mm (= L), in respect (Fig. 5a). This geometry is taken to induce the stress concentration around the notch tip.

Table 2. Size-independent and size-dependent mechanical properties of float glass and cement mortar.
Tabela 2. Dimenziono nezavisne i zavisne mehaničke osobine flot stakla i cementnog maltera.

Mechanical properties	Float glass	Cement mortar
Young's modulus, E (GPa)	58	20
Poisson's ratio, ν (-)	0.218	0.28
Ultimate tensile strength, σ_{UTS} (MPa)	46.70	7.5
Characteristic length scale, L_c=L_G (mm)	10^{-6}	1
Cosserat couple modulus, μ_c (GPa)	μ_c=μ=E/2(1+ν)	μ_c=μ=E/2(1+ν)

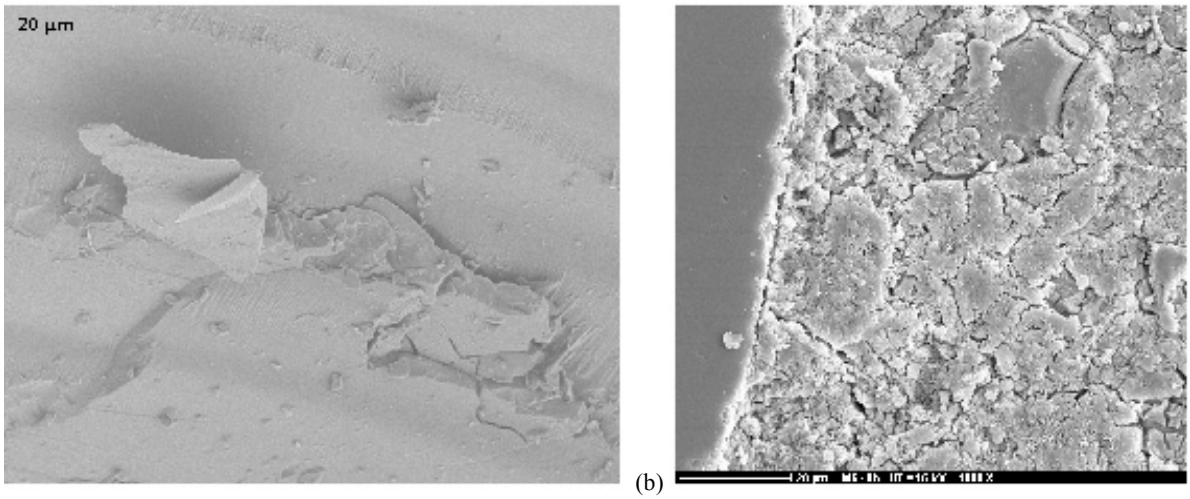

(a) (b)

Figure 4. SEM images of chosen materials a) Float glass, b) Cement mortar 48 hours after hydration process.
Slika 4. SEM slike izabranih materijala (flot staklo i cementni malter), a) flot staklo, b) cementni malter 48 sati posle hidratacije.

Hence, these Modified Brazilian Disk (MBD) samples will be broken using the notch tip crack concept /80/. This is absolutely very good wayout in tensile strength evaluation of elastic brittle materials. This trims off the interferences among boundary conditions and high concentration zones at notch root (contact problem), i.e. central hole of the MBD samples.

The 3D-FEM implementations have been made by the isoparametric quadratic and linear Lagrange shape functions for displacement and micro-rotation vectors ($u \in \mathbb{R}^3$ and $\phi \in \mathbb{R}^3$), respectively. The main advantage of this choice is to obtain very stable mesh-independency problem as well as low computation costs, i.e. they are computationally affordable and rather exact. All computations are done by the Geometric Multi-Grid (GMG) solver well-known as an iterative solver including the parallelization of non-symmetric systems. The major advantage of the above-mentioned solver is its ability to handle very large Cosserat models. This matter gets more crucial when we would like to solve non-linear generalized continuum media. In these cases, more DOFs should be expected at every node comparing to the classical theory and consequently, direct solvers efficiency becomes less colourful for huge DOFs (Fig. 5c). In Table 3, mesh statistics of the 3D-FEM model of MBD samples are given. It is essential to mention that boundary conditions for the micro-rotation vector are still open problems. Some groups call them as the artificial boundary conditions and they insist on the fact that one should not provide any boundary conditions in conjunction with the micro-rotations. Unlikely, other groups imply these kinds of boundary conditions for micro-rotations. This is neatly performed for the microstretch theory by Kirchner and Steinmann in their landmark work /81/. They have substantiated that lack of the micro-rotation boundary conditions induces a constant micro-rotation field. In the current work, this methodology is followed throughout the numerical computations.

Numerical simulation results and discussion

In this sub-section, we investigate the impact of the characteristic length which has been presumably considered as mean value of the grains diameter ($L_{c1} = L_{c2} = L_{c3} = L_G$). We take into account two different materials, i.e. glass and cement mortar. The float glass is well known as a non-granular material (amorphous material). An interesting consequence of this choice is that the characteristic length scale must be nearly zero or zero ($L_c \rightarrow 0$). In this case, the

Cosserat theory reduces to one kind of classical theory (Cauchy-Boltzmann theory). In the meanwhile the micro-rotation vector reaches very small values relative to the cement mortar. Considering the cement mortars as highly porous materials including the aggregates and independent micro-rotation concept which is explicitly built in the Cosserat-based media, we find out relatively high micro-rotation values. As a matter of fact, the Cosserat-theory not only handles the classical theories ($L_c = 0$ and $\mu_c = 0$) but also it promises an explicit methodology to treat the granular materials.

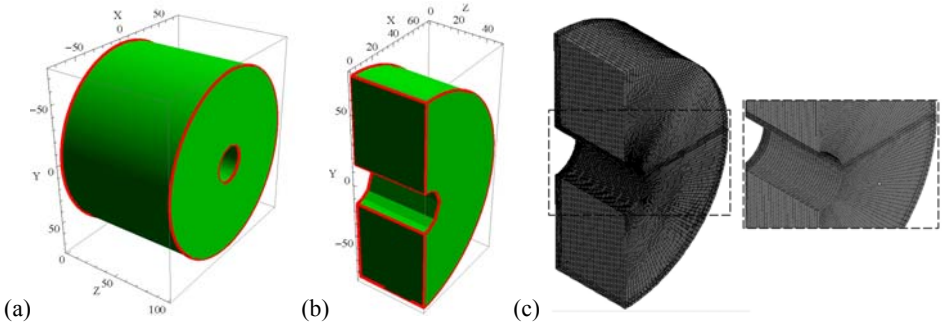

(a) (b) (c)

Figure 5. Illustration of the Modified Brazilian Disk (MBD) specimens (outside diameter=150 mm, inside diameter=30 mm and thickness=100 mm), a) Geometrical configuration of chosen MBD specimen for FEM experiments, b) One-quarter symmetry assumption using median plane and its normal plane as symmetry planes, c) Mesh density of chosen MBD specimen (Element type= hexahedral 28-node solid element, DOFs=4605903 including Lagrange multiplier DOFs).

Slika 5. Prikaz epruvete Modifikovanog brazilskog diska (MBD) (spoljni prečnik=150 mm, unutrašnji prečnik=30 mm i debljina=100 mm), a) geometrijska konfiguracija epruvete MBD za FEM eksperimente, b) pretpostavka četvrtine simetrije korišćenjem srednje ravni i njene normalne ravni kao ravni simetrije, c) gustina mreže MBD epruvete (tip elementa=puni heksaedar sa 28 čvorova, stepeni slobode=4605903 zajedno sa Lagranžovim koeficijentima stepeni slobode)

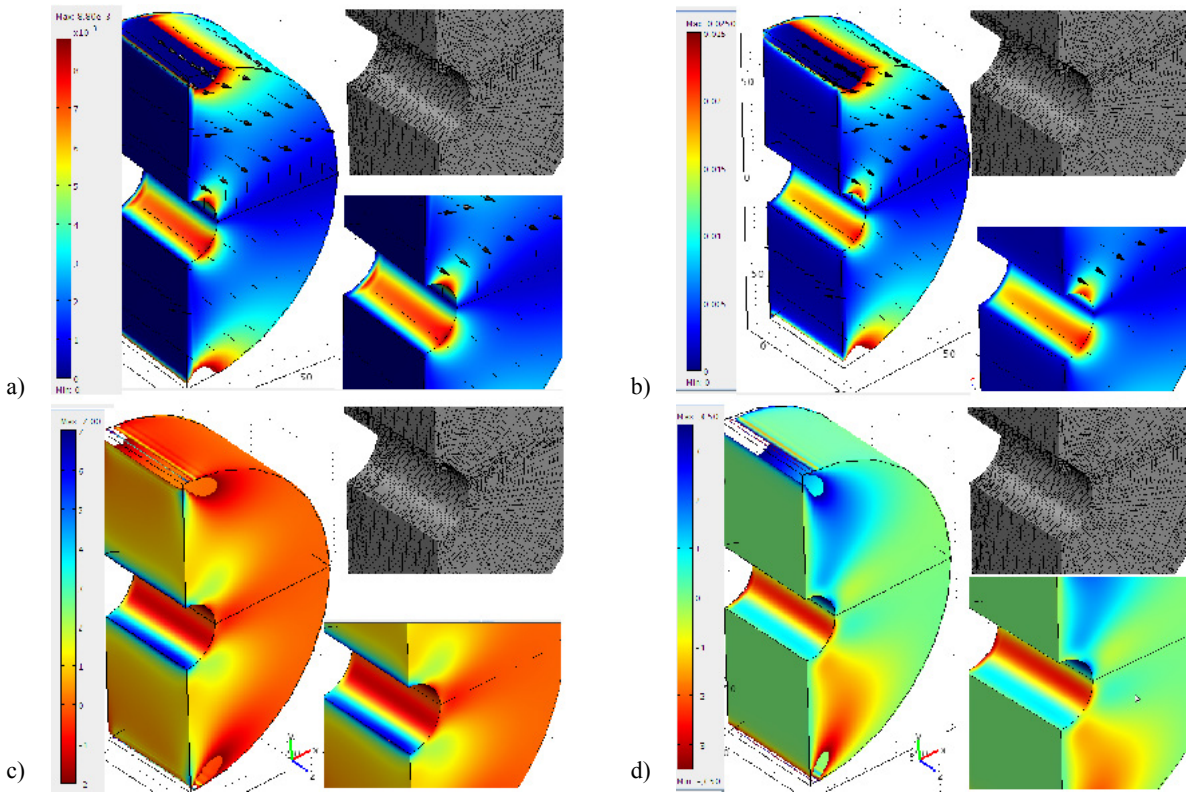

a) b) c) d)

Figure 6. Non-linear Cosserat outcomes for float glass and cement mortar under indirect tensile test via the Modified Brazilian Disk (MBD) specimens (compressive force=10 kN), a) Norm of micro-rotation vector ($\|\phi\|$) or micro-rotation vector magnitude in degree including micro-rotation vector field (black arrows) for float glass (maximum value around the central hole=8.8×10^{-3} (°), b) Norm of micro-rotation vector ($\|\phi\|$) or micro-rotation vector magnitude in degree including micro-rotation vector field (black arrows) for cement mortar (maximum value around the central hole=25×10^{-3} (°), c) Normal stress component in x direction (σ_{xx}) in MPa, d) Shear stress component in xy plane (σ_{xy})

Slika 6. Nelinearna Kosera rešenja za flot staklo i cementni malter u indirektnom ispitivanju zatezanjem MBD epruveta (pritisna sila=10 kN), a) Normirani vektor mikrorotacije ($\|\phi\|$) ili intenzitet vektora mikrorotacije u stepenima zajedno sa poljem vektora mikrorotacije (crne strelice) za flot staklo (najveća vrednost je oko centralnog otvora=8.8×10^{-3} (°), b) Normirani vektor mikrorotacije ($\|\phi\|$) ili intenzitet vektora mikrorotacije u stepenima zajedno sa poljem vektora mikrorotacije (crne strelice) za cementni malter (najveća vrednost je oko centralnog otvora=25×10^{-3} (°), c) Normalna komponenta napona u x pravcu (σ_{xx}) u MPa, d) Komponenta napona smicanja u xy ravni (σ_{xy}) u MPa.

Table 3. Mesh statistics and 3D-FEM model assumptions for the non-linear Cosserat computations.
Tabela 3. Statistika mreže i 3D-FEM pretpostavke modela za nelinearni proračun Kosera.

Element type	Element No.	FEM symmetry	DOFs
Quadratic and linear for $u \in \mathbb{R}^3$ and $\phi \in \mathbb{R}^3$	165000	one-quarter	4.606 Mi

Another feature which can be basically found out from the numerical computations is that the stress localization is less colourful in the Cosserat theory compared to the classical one /82-84/. This matter can be interpreted by the fact that there is the energy equality feature. Hence, one part of applied actions, e.g. forces and moments would be distributed through the strain energy density and another counterpart would be used to undertake the curvature energy density. This issue is well-known and it well agrees with the reality of the granular and heterogeneous materials. Correspondingly, the weak shear stress value is obtained near the central hole of the MBD 3D-FEM models. It is obvious that the symmetric stress moment ($m \in \mathrm{sym}(3) \subset \mathbb{R}^3 \times \mathbb{R}^3$) might be expected due to the equality of β and γ like case2. The numerical experiments substantiate this matter, i.e. $m_{ij} = m_{ji}$. However, the stress tensor is still asymmetric second-rank tensor and its skew-symmetric counterpart provides the stress moment tensor. Therefore, the amount of the stress moment tensors unavoidably depends on the shear stresses and the actions which significantly produce them, e.g. pure torsion test or pure shear test commonly used to investigate the shear effects in classical mechanics. To exemplify this issue, we refer the landmark studies of Gauthier and Jahsman /35/ and Gauthier himself /75/. More recent investigation would be also addressed in /64/.

SUMMARY, CONCLUSION AND OUTLOOK

The numerical experiments of non-linear Cosserat theory have been performed on the brittle materials under indirect tensile strength experiments well-known as Modified Brazilian Disk (MBD). This sort of tensile strength assessment experiments is successfully applied into the brittle materials in predicting their tensile strength. This also avoids any other side-effects which simultaneously occur through the brittle samples during the test procedure. The presence of the central hole neatly wipes out these effects and results in quite well tensile strength estimation for brittle elastic materials. To achieve the non-linear Cosserat numerical experiments herein, three main assumptions are taken into account:

1. The material moduli, i.e. α, β, and γ, which link the stress moment tensor to the curvature tensor or so-called wryness tensor in the second constitutive law of the Cosserat-based media, are considered in function of the microstructure state, notably the grain size,
2. The characteristic length scale L_c is considered as an average grain diameter ($L_c := L_G$). The ellipsoid grains with three different diameters and random orientations are primarily accounted for. Using the identical characteristic length scales for the aforementioned grains, the spherical ones are created.
3. According to the physical and mathematical restrictions on the Cosserat-based media as generalized continuum media, parameter μ_c is customarily fixed to μ. As pointed out previously, $L_c = 0$ and $\mu_c = 0$ yield the classical theory. The fact that we take $\mu_c = \mu$ is beneficial in the sense that it still stands for the Cosserat media whatever L_c values. Furthermore, it is computationally affordable while we are in front of enormous amount of DOFs, particularly for the non-linear Cosserat theory.

Based upon above-mentioned assumptions, the computations have been carried out for our selected materials. We have willingly chosen these materials, i.e. glass and mortar cement. They represent two extremely different micro-structures, i.e. amorphous and heterogeneous micro-structures. Using the numerical outcomes, one can readily realize that the amorphous materials are extremely close to the classical theory of elasticity, whereas the granular materials provoke one kind of independent rotation whose effect can be neatly covered in an explicit manner via the Cosserat theory. In the case of granular materials, these effects are entirely clear and obvious. Therefore, more micro-rotation and less stress localization would be expected for these materials. L_c value has a great impact on these independent micro-rotations which are promised under Cosserat theory. This would be a fresh route for material modelling of the heterogeneous materials. Nevertheless, some salient open problems still remain:

- The first is the micro-rotation boundary conditions issue, one can ask himself whether or not these boundary conditions would be taken into account (grid-framework boundary conditions versus artificial boundary conditions),
- The second one is μ_c called Cosserat couple modulus. According to the generalized continuum theory, very small μ_c values make us closer to the classical theory, whereas the large μ_c, i.e. $\mu_c \to \infty$ coincides with the couple stress theory or so-called indeterminate couple stress theory /8, 9, 85/. Although, these case limits or penalized cases are pretty well-known, the physical meaning of this material modulus is still an open problem.

ACKNOWLEDGEMENTS

The authors thank Prof. P. Neff who provided some very fruitful comments and suggestions about the non-linear Cosserat theory. The authors also thank Prof. S. Forest for his valuable remarks about the generalized continuum mechanics during our meeting held at Ecole des Mines de Paris in Paris last summer.

REFERENCES

1. Cosserat, E. Cosserat, F., *Théorie des corps déformables.* Librairie Scientifique A. Hermann et Fils (engl. translation by D. Delphenich 2007, pdf available at http://www.mathematik.tudarmstadt.de/fbereiche/analysis/pde/staff/neff/patrizio/Cosserat.html), Paris, 1909.
2. a) Günther, W., *Zur statik und kinematik des cosseratschen kontinuums*. Abh. Braunschweig Wiss. Ges., 10:195-213, 1958. (In German). b)

3. Eringen, A.C., Suhubi, E.S., *Nonlinear theory of simple micro-elastic solids*. Int. J. Eng. Sci., 2:189-203, 1964.
4. Green, A.E., Rivlin, R.S., *Multipolar continuum mechanics*. Arch. Rat. Mech. Anal., 17:113-147, 1964.
5. Cowin, S., *An incorrect inequality in micropolar elasticity theory*. Z. Angew. Math. Physik, 21:494-497, 1970.
6. Eringen, A.C., Kafadar, C.B., *Polar Field Theories*. In A.C. Eringen, editor, Continuum Physics, volume IV: Polar and Nonlocal Field Theories, pages 1-73. Academic Press, New York, 1976.
7. Eringen, A.C., *Microcontinuum Field Theories*. Springer, Heidelberg, 1999.
8. Toupin, R.A., *Elastic materials with couple stresses*. Arch. Rat. Mech. Anal., 11:385-413, 1962.
9. Mindlin, R.D., *Influence of couple-stresses on stress concentrations*. Experimental Mechanics, 3(1):1-7, 1963.
10. Ristinmaa, M., Vecchi, M., *Use of couple-stress theory in elasto-plasticity*. Comp. Meth. Appl. Mech. Engng., 136:205-224, 1996.
11. Alshibli, K.A., Alsaleh, M.I., Voyiadjis, G.Z., *Modelling strain localization in granular materials using micropolar theory: mathematical formulations*. Int. J. Num. Anal. Meth. Geomech., 30(15):1501-1524, 2006.
12. Alshibli, K.A., Alsaleh, M.I., Voyiadjis, G.Z., *Modelling strain localization in granular materials using micropolar theory: numerical implementation and verification*. Int. J. Num. Anal. Meth. Geomech., 30(15):1525-1544, 2006.
13. Vardoulakis, I., *Shear-banding and liquefication in granular materials on the basis of a cosserat theory*. Ingenieur-Archiv, 59:106-114, 1989.
14. de Borst, R., *Simulation of strain localization: a reappraisal of the Cosserat continuum*. Engng. Comp., 8:317-332, 1991.
15. de Borst, R., Sluys, L.J., *Localization in a Cosserat continuum under static and loading conditions*. Comp. Meth. Appl. Mech. Engng., 90:805-827, 1991.
16. de Borst, R., *A generalization of J_2-flow theory for polar continua*. Comp. Meth. Appl. Mech. Engng., 103:347-362, 1992.
17. Iordache, M.M., Willam, K., *Localized failure analysis in elastoplastic cosserat continua*. Comp. Meth. Appl. Mech. Engng., 151(3-4):559-586, 1998.
18. Bauer, E., *Analysis of shear band bifurcation with a hypoelastic model for a pressure and density sensitive granular material*. Mechanics of Materials, 31(9):597-609, 1999.
19. Tejchman, J., Gudehus, G., *Shearing of a narrow granular layer with polar quantities*. Int. J. Num. Anal. Meth. Geomech., 25(1):1-28, 2001.
20. Manzari, M.T., *Application of micropolar plasticity to post failure analysis in geomechanics*. Int. J. Num. Anal. Meth. Geomech., 28(10):1011-1032, 2004.
21. Maier, Th., *Comparison of non-local and polar modelling of softening in hypoplasticity*. Int. J. Num. Anal. Meth. Geomech., 28(3):2004, 2004.
22. Bardet, J.P., Proubet, J., *A numerical investigation of the structure of persistent shear band in granular media*. Géotechnique, 41(4):599-613, 1992.
23. Bardet, J.P., Proubet, J., *A shear band analysis in idealized granular materials*. J. Engng. Mech., ASCE, 118(2):397-415, 1992.
24. Diebels, S., Steeb, H., *The size effect in foams and its theoretical and numerical investigation*. Proc. R. Soc. London A, 458:2869-2883, 2002.
25. Diebels, S., Steeb, H., *Stress and couple stress in foams*. Comp. Mat. Science, 28:714-722, 2003.
26. Neff, P., Forest, S., *A geometrically exact micromorphic model for elastic metallic foams accounting for affine microstructure. Modelling, existence of minimizers, identification of moduli and computational results*. J. Elasticity, 87:239-276, 2007.
27. Tekoglu, C., Onck, P.R., *Size effects in two-dimensional voronoi foams: A comparison between generalized continua and discrete models*. Journal of the Mechanics and Physics of Solids, 56(12):3541-3564, 2008.
28. Tekoglu, C., Size effect in cellular solids. PhD thesis, Rijksuniversiteit, Netherlands, 2007.
29. Zhang, H.W., Wang, H., Wriggers, P., Schrefler, B.A., *A finite element method for contact analysis of multiple cosserat bodies*. Comput. Mech., 36(6):444-458, 2005.
30. Zhang, H.W., Wang, H., Chen, B.S., Xie, Z.Q., *Analysis of cosserat materials with voronoi cell finite element method and parametric variational principle*. Comp. Meth. Appl. Mech. Engng., 197(6-8):741-755, 2008.
31. Riahi, A., Curran, J.H., *Full 3d finite element cosserat formulation with application in layered structures*. Applied Mathematical Modelling, 33(8):3450-3464, 2009.
32. Desrues, J., Localisation de la déformation plastique dans les matériaux granulaires. PhD thesis, University of Grenoble, 1984. (In French).
33. Lakes, R.S., *Experimental microelasticity of two porous solids*. Int. J. Solids Struct., 22(1):55-63, 1986.
34. Gauthier, R.D., Jahsman, W.E., *A quest for micropolar constants*. ASME J. Appl. Mech., 42:369-374, 1975.
35. Gauthier, R.D., Jahsman, W.E., *Bending of a curved bar of micropolar elastic material*. ASME J. Appl. Mech., 43:502-503, 1976.
36. Bazant, Z.P., Christensen, M., *Analogy between micropolar continuum and grid frameworks under initial stress*. Int. J. of Solids and Structures, 8(3):327-346, 1972.
37. Pijaudier-Cabot, G., Bazant, Z.P., *Non local damage theory*. J. Engng. Mech., ASCE, 113(10):1512-1533, 1987.
38. Bazant, Z.P., Pijaudier-Cabot, G., *Measurement of characteristic length of non local continuum*. J. Engng. Mech., ASCE, 115(4):755-767, 1989.
39. Iesan, D., *Torsion of micropolar elastic beams*. Int. J. Eng. Sci., 9:1047-1060, 1971.
40. Park, H.C., Lakes, R.S., *Torsion of a micropolar elastic prism of square cross section*. Int. J. Solids Struct., 23:485-503, 1987.
41. Jeong, J., Adib, H., Pluvinage, G., *Proposal of new damage model for thermal shock based on dynamic fracture on the brittle materials*. Journal of Non-Crystalline Solids, 351(24-26):2065-2075, 2005.
42. Neff, P., Jeong, J., Münch, I., Ramézani, H., *Mean field modeling of isotropic random Cauchy elasticity versus microstretch elasticity*. Z. Angew. Math. Phys., 60(3):479-497, 2009.
43. Wu, H.-C., Continuum mechanics and plasticity. Chapman and Hall/CRC Press, 2005.
44. Pietraszkiewicz, W., Eremeyev, V.A., *On natural strain measures of the non-linear micropolar continuum*. International Journal of Solids and Structures, 46(3-4):774-787, 2009.
45. Pietraszkiewicz, W., Eremeyev, V.A., *On vectorially parameterized natural strain measures of the non-linear cosserat continuum*. International Journal of Solids and Structures, 46(11-12):2477-2480, 2009.
46. Rooney, J., *A survey of representations of spatial rotation about a fixed point*. Environment and Planning B, 4(2):185-210, 1977.
47. Guo, Z.-H., *Representations of orthogonal tensors*. Solid Mechanics Archives, 6(4):451-466, 1981.
48. Pietraszkiewicz, W., Badur, J., *Finite rotations in the description of continuum deformation*. International Journal of Engng. Science, 21(9):1097-1115, 1983.

49. Altman, S.L., Rotations, Quaternions, and Double Groups. Clarendon Press Oxford, 1986.
50. Atluri, S.N., Cazzani, A., *Rotations in computational solid mechanics*. Achieves of Computational Mechanics and Engng., 2(1):49-138, 1995.
51. Borri, M., Bottasso, C.L., Trainelli, L., *On representations and parameterizations of motion*. Multibody System Dynamics, 4(2-3):129-193, 2000.
52. Geradin, M., Cardona, A., Flexible Multibody Dynamics: A Finite Element Approach. Wiley, Chichester, 2001.
53. Chroscielewski, J., Makowski, J., Pietraszkiewicz, W., powłok wielopłatowych. Nieliniowa teoria i metoda elementów skon' czonych Wydawnictwo Statyka i dynamika. IPPT PAN, Warszawa, 2004. (in Polish).
54. Münch, I., Wagner, W., Neff, P., *Constitutive modeling and FEM for a nonlinear cosserat continuum*. PAMM, 6(1):499-500, 2006.
55. Münch, I., Ein geometrisch und materiell nichtlineares Cosserat-Modell-Theorie, Numerik und Anwendungsmöglichkeiten. PhD thesis, University of Karlsruhe (TH), October 2007. (In German).
56. Sansour, C., Skatulla, S., *A non-linear Cosserat continuum-based formulation and moving least square approximations in computations of size-scale effects in elasticity*. Computational Mat. Sci., 41(4):589-601, 2008.
57. Donea, J., Huerta, A., Ponthot, J.-Ph., Rodrıguez-Ferran, A., Encyclopedia of Computational Mechanics, volume 1, Fundamentals, Chapter 14. John Wiley and Sons, 2004.
58. Jeong, J., Neff, P., *Existence, uniqueness and stability in linear Cosserat elasticity for weakest curvature conditions*. Mathematics and Mechanics of Solids, 15(1):78-95, 2010. First published on Sep. 17, 2008, doi:10.1177/1081286508093581.
59. Lakes, R.S., *A pathological example in micropolar elasticity*. ASME J. Appl. Mech., 52:234-235, 1985.
60. Anderson, W.B., Lakes, R.S., *Size effects due to Cosserat elasticity and surface damage in closed-cell polymethacrylimide foam*. J. Mat. Sci., 29:6413-6419, 1994.
61. Neff, P., *The Cosserat couple modulus for continuous solids is zero viz the linearized Cauchy-stress tensor is symmetric*. Preprint 2409, http://www3.mathematik.tudarmstadt.de/fb/mathe/bibliothek/preprints.html , Z. Angew. Math. Mech., 86:892-912, 2006.
62. Ramézani, H., Jeong, J., *A novel linear cosserat elasticity models with grid framework model assumptions: 3d numerical experiments of the torsion test*. International Journal of Mechanical Sciences, May 2009. Submitted.
63. Neff, P., Jeong, J., *A new paradigm: the linear isotropic Cosserat model with conformally invariant curvature energy*. Z. Angew. Math. Mech., 89(2):107-122, 2009.
64. Neff, P., Jeong, J., Fischle, A., *Stable identification of linear isotropic cosserat parameters: bounded stiffness in bending and torsion implies conformal invariance of curvature*. Acta Mechanica, 211(3):237-249, May 2010.
65. Jeong, J., Ramézani, H., Münch, I., Neff, P., *Simulation of linear isotropic Cosserat elasticity with conformally invariant curvature*. Z. Angew. Math. Mech., 89(7):552-569, 2009.
66. Jeong, J., Ramézani, H., *Implementation of the finite isotropic linear cosserat models based on the weak form*. In Scientific committee of European Comsol Conference in Hannover-Germany, editor, European Comsol Users Conference 2008, November 2008.
67. Lakes, R.S., *On the torsional properties of single osteons*. J. Biomech., 25:1409-1410, 1995.
68. Zastrau, B., *Zur Berechnung orientierter Kontinua - Entwicklung einer Direktorentheorie und Anwendung der Finiten Elemente*. Number 4/60 in Fortschrittberichte der VDI Zeitschriften. Verein Deutscher Ingenieure, VDI-Verlag GmbH, Düsseldorf, 1981.
69. Zastrau, B., Rothert, H., Herleitung einer Direktortheorie für Kontinua mit lokalen Krümmungseigenschaften. Z. Angew. Math. Mech., 61:567-581, 1981.
70. de Borst, E., *Simulation of strain localisation: a reappraisal of the cosserat continuum*. Eng. Comput., 8(4):317-332, 1991.
71. Forest, S., Dendievel, R., Canova, G.R., *Estimating the overall properties of heterogeneous Cosserat materials*. Modelling Simul. Mater. Sci. Eng., 7:829-840, 1999.
72. Neff, P., Jeong, J., Ramézani, H., *Subgrid interaction and micro-randomness - novel invariance requirements in infinitesimal gradient elasticity*. International Journal of Solids and Structures, 46(25-26):4261-4276, 2009.
73. Neff, P., Jeong, J., Münch, I., Ramézani, H., Linear Cosserat Elasticity, Conformal Curvature and Bounded Stiffness. In G.A. Maugin and V.A. Metrikine, editors, Mechanics of Generalized Continua. One hundred years after the Cosserats, volume 21 of Advances in Mechanics and Mathematics, pages 55-63. Springer, Berlin, 2010.
74. Neff, P., Münch, I., *Curl bounds Grad on SO(3)*. Preprint 2455, http://www3.mathematik.tudarmstadt.de/fb/mathe/bibliothek/preprints.html , ESAIM: Control, Optimisation and Calculus of Variations, published online, DOI: 10.1051/cocv:2007050, 14(1):148{159, 2008.
75. Gauthier, R.D., Experimental investigations on micropolar media. In O. Brulin and R.K.T. Hsieh, editors, Mechanics of Micropolar Media, pages 395-463. CISM Lectures, World Scientific, Singapore, 1982.
76. Bazant, Z.P., Chang, T.P., *Instability of nonlocal continuum and strain averaging*. J. Engng. Mech., 110:1441-1450, 1984.
77. Forest, S., Pradel, F., Sab, K., *Asymptotic analysis of heterogeneous cosserat media*. International Journal of Solids and Structures, 38(26-27):4585-4608, 2001.
78. Hongwu, Z., Hui, W., Biaosong, C., Zhaoqian, X., *Parametric variational principle based elastic-plastic analysis of cosserat continuum*. Acta Mechanica Solida Sinica, 20(1):65-74, 2007.
79. Jeong, J., Adib-Ramezani, H., *Effect of specimen shape on the behavior of brittle materials using probabilistic and deterministic methods*. Journal of the European Ceramic Society, 26(16):3621-3629, 2006.
80. Atkinson, C., Smelser, R.E., Sanchez, J., *Combined mode fracture via the cracked brazilian disk test*. International Journal of Fracture, 18(4):279-291, April 1982.
81. Kirchner, N., Steinmann, P., *Mechanics of extended continua: modeling and simulation of elastic microstretch materials*. Computational Mechanics, 40(4):651-666, 2007.
82. Nakamura, S., Lakes, R.S., *Finite element analysis of stress concentration around a blunt crack in a cosserat elastic solid*. Comp. Meth. Appl. Mech. Engng., 66(3):257-266, 1988.
83. Lakes, R.S., Nakamura, S., Behiri, J.C., Bonfield, W., *Fracture mechanics of bone with short cracks*. J. Biomechanics, 23(10): 967-975, 1990.
84. Jeong, J., Ramézani, H., Benboudjema, F., *Numerical implementation of the deformation of drying shrinkage of the cement-based materials: Effect of micro structure -cauchy's approach or second gradient approach?* In Scientific committee of European Comsol Conference, Milan-Italy (http://www.comsol.eu/conference2009/europe/papers/), editor, European Comsol Users Conference 2009, 14-16 Oct. 2009.
85. Mindlin, R.D., Tiersten, H.F., *Effects of couple stresses in linear elasticity*. Arch. Rat. Mech. Anal., 11:415-447, 1962.